PCCP

PAPER

View Article Online
View Journal

Cite this: DOI: 10.1039/c7cp07024a

Visible light driven plasmonic photochemistry on nano-textured silver

Jaspreet Walia,*[ab] Jean-Michel Guay,[ac] Oleksiy Krupin,[ad] Fabio Variola,[b] Pierre Berini[acd] and Arnaud Weck[abc]

Received 14th October 2017,
Accepted 28th November 2017

DOI: 10.1039/c7cp07024a

rsc.li/pccp

Plasmon assisted generation of silver sulfate from dodecanethiol is demonstrated on a nano-textured silver substrate with a strong surface plasmon resonance in the visible range. The observed photo-physical processes are attributed to hot charge carriers that are generated from the excitation of surface plasmon resonances using 532 nm laser light. Excited charge carriers are responsible for cleaving the alkane chain, and for generating reactive oxygen species which rapidly photooxidize the exposed sulfur atoms. The ability to drive photochemical reactions with photon energies in the visible range rather than in the UV, on nano-textured silver surfaces, will enable researchers to study photochemical transformations for a wide variety of applications. The strong optical absorbance across the visible range, combined with the fact that the substrates can be fabricated over large areas, naturally makes them candidates for solar driven photochemical applications, and for large scale plasmonic reactors.

Introduction

Our current understanding of surface plasmon resonances (SPR) on gold (Au) and silver (Ag), combined with the recent surge in realizing various noble metal nanostructures has generated interest in both academia and industry that is focussed on real-world applications. The type of metal, geometry, and surrounding environment all influence the wavelength which generates maximum excitation of SPR. The classic examples of size dependant plasmon resonances are nanoparticles in solution. The shift in resonance resulting from a change in refractive index at the surface has found considerable success when used for molecular detection on nano-textured metals.[1–5]

More recently, plasmon assisted photochemistry on nano-textured metal surfaces has received considerable attention.[6–12] On resonance, very strong electric fields are generated near nano-textured features, and even stronger fields have been reported in gaps between nanostructures.[13–16] The metal regions where significant electric field enhancement occurs also contain an elevated density of excited charge carriers, which in turn can be used to drive photo-physical processes in adsorbed molecules. Charge transfer can occur *via* tunneling processes, where charge carriers are transferred to/from frontier orbitals in the adsorbate. When considering charge transfer dynamics between metallic surfaces and molecules (*e.g.*, a metal–organic interface), self-assembled monolayers (SAM) of alkanethiols on highly conductive substrates represents a good model system. Scanning tunneling microscopy,[17–19] and conducting probe force microscopy[20] experiments are usually performed to determine the position of the Fermi level in a metal relative to the highest occupied molecular orbital (HOMO) and lowest unoccupied molecular orbital (LUMO).[21] Although these measurements provide a consistent value for the HOMO–LUMO gap in alkanethiols, the position of the Fermi level remains under debate, and therefore it is unknown if tunneling processes are dominated by holes or electrons.

In this study, the formation of silver sulfate (Ag_2SO_4) *via* CW visible laser irradiation of a dodecanethiol ($HS[CH_2]_{10}CH_3$) layer on nano-textured Ag in air is reported. The surfaces are nano-textured using picosecond laser pulses, which generate spherical nanoparticles of varying sizes and SPR throughout the visible range. Previously, it was shown that by varying the fabrication parameters, many different colours could be produced on silver surfaces.[22] In the past, photooxidation of dodecanethiol was observed in samples irradiated by UV photon energies,[23–28] and significant progress has been made in connection with UV photo-patterning of alkanethiol monolayers for various biological and chemical applications.[29–32] Here, we demonstrate that a 532 nm (2.33 eV) source producing an output power of 0.5 mW can drive the formation of sulfate species from an alkanethiol monolayer formed onto a nano-textured Ag surface that generates strong SPR in the visible. During laser irradiation, acquired Raman spectra clearly reveal the formation of R-SO_4^{2-} units,

[a] Centre for Research in Photonics, University of Ottawa, Ontario, Canada. E-mail: jwalia@uottawa.ca
[b] Department of Mechanical Engineering, University of Ottawa, Ontario, Canada
[c] Department of Physics, University of Ottawa, Ottawa, Ontario, Canada
[d] School of Electrical Engineering and Computer Science, University of Ottawa, Ottawa, Ontario, Canada

purported to be Ag_2SO_4, consistent with other views.[23,33,34] We conclude that hot carriers, efficiently generated within silver nanostructures near the surface due to strong coupling of the incident light to SPR modes thereon, are responsible for the observed photochemical transformations.

The demonstration that chemical reactions on large-area nano-textured silver surfaces can be driven by 0.5 mW of visible laser radiation represents a significant step towards realizing new photochemical reactors for potential industrial use. In this connection, catalytic oxidation reactions are of interest. Namely the partial oxidation of ethylene to form ethylene oxide. Furthermore, UV radiation can be hazardous to work with, and requires special optics and materials to perform experiments, driving up costs. The ability to photooxidize alkanethiols using visible light rather than UV light will now enable researchers to examine photooxidation and photo-patterning of thiols for a wide variety of biochemical applications.

Sample fabrication

High purity (99.99%) silver samples approximately 4 mm thick and 38 mm in diameter were obtained from the Royal Canadian Mint (Ottawa, Canada). Nanotexturing of the silver surfaces was recently reported, and a detailed account of the process is available in the literature.[22,35] Briefly, we used a 15 W Duetto (Nd:YVO4, Time-Bandwidth Product) mode-locked MOPA pulse-burst laser at the fundamental wavelength of 1064 nm, operating at a fixed frequency of 25 kHz. The time separation between each of the pulses contained within a burst is fixed at 12.8 ns. The energy distribution of each pulse contained within a burst was controlled using FlexBurst™. An F-theta lens (f = 254 mm, Rodenstock) was used to focus the light to a measured spot size of 28 μm. The spot size was determined from semilogarithmic plots of the modified regions as described in the literature.[22,36] The samples were placed on a 3-axis translation stage with a resolution of 1 μm on each of the individual axis. Each sample was raster scanned in a top to bottom pattern using galvanometric mirrors (TurboScan, Raylaser) at a speed of 150 mm s^{-1}.

To modify the surfaces of the nano-textured silver, samples were immersed in a 2 mM solution of 1-dodecanethiol, $HS[CH_2]_{11}CH_3$ dissolved in IPA for 3 hours. To avoid the formation of multilayer alkanethiols at the surface, the sample was thoroughly washed by placing it in three separate IPA baths for 20 minutes each. After each immersion, the sample was agitated for approximately 2 minutes to allow un-reacted alkanethiol molecules to diffuse out into the IPA solution. All the experiments were carried out in glass (Pyrex) Petri dishes.

RAIRS and Raman measurement

Grazing angle IR measurements were performed on a Thermo Nicolet Nexus 870 FT-IR spectrometer with the incident light beam hitting the surface of the sample at 86°. Raman spectroscopic data was recorded using a WiTec Alpha a300 system in the backscattering configuration, at an incident wavelength of 532 nm, focused through a 20 × 0.4 N.A. objective. Photooxidation was initiated using an irradiance of 15 kW cm^{-2} in ambient conditions. During photooxidation, spectra were acquired using an integration time of 2 s, and 3 accumulations were averaged. Spectra were taken at 1 minute intervals for 60 minutes.

Results

The plasmonic nature of the substrate is readily seen in the images of Fig. 1. The topography and the structural colour generated by the surface are clearly observed in the bright-field microscope image of Fig. 1(a). The surface consists of nanoparticle clusters scattered over underlying laser-induced periodic surface structures (LIPSS), as observed in the SEM image of Fig. 1(b), resulting in the generation of the blue/gold hues observed in Fig. 1(a) and its inset which shows a photograph of the surface as perceived by the naked eye. The measured reflectance spectrum covering the 300 to 800 nm range is plotted in Fig. 1(c), and shows that there is a significant increase in the amount of light absorbed in this range relative to bulk silver

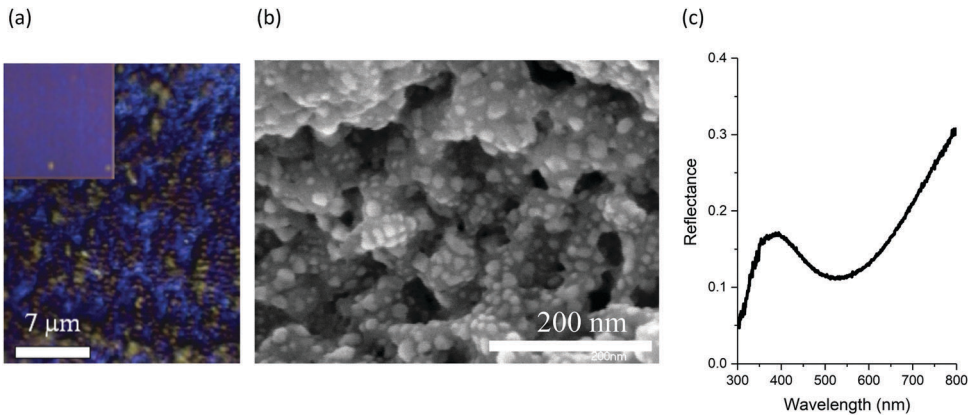

Fig. 1 (a) Nano-textured silver producing a blue hue due to plasmonic resonances that are excited in ambient light; image taken with a bright field microscope at 100× magnification. The inset is a photograph of the surface as seen by the naked eye. (b) SEM image showing the highly topographical nature of the surface after the laser machining process. (c) Corresponding measured reflectance spectrum displaying a strong plasmonic resonance centred at ~530 nm. The peak in reflectance centred at ~400 nm is responsible for producing the blue hue perceived in (a).

which has near unity reflectance over the visible range. More importantly, the spectrum displays a maximum absorbance at ~530 nm, a peak in reflectance at ~400 nm, and a gradually increasing reflectance throughout the yellow and red regions of the visible spectrum. These features are consistent with the colours observed in Fig. 1(a). Moreover, the spectral line shape observed in Fig. 1(c) is indicative of a plasmonic resonance. The mechanisms responsible for rendering colours on similar surfaces has been discussed in detail previously.[22,36] The most salient feature is the highly absorptive nature of this silver surface, where less than 25% reflectance is seen over the 400–800 nm range, with values decreasing to as low as 10% on resonance. Another interesting feature of these surfaces is the colour perceived by the naked eye does not depend on viewing angle.

To confirm the presence of dodecanethiol on the surface, a grazing angle IR absorbance spectrum was recorded and is shown in Fig. 2. A background spectrum was recorded from a coloured silver surface that was maintained under the same conditions. Emphasis was given to the 3050–2750 cm^{-1} spectral region, where the strongest IR absorbance bands in dodecanethiol occur and are associated with C–H stretching vibrations. The assignment of specific vibrational modes of various alkanethiols in this spectral region has been reported previously.[37–40] There are nine vibrational modes that can potentially be observed, all corresponding to CH vibrations in the methylene chain and methyl headgroup. Spectral deconvolution of the data was performed to accurately determine the center frequency positions of the various peaks, and is also shown in Fig. 2. Center frequencies for the symmetric and asymmetric CH stretching vibrations in the methylene groups were assigned values of $\nu_s(CH_2)$ = 2848 cm^{-1} and $\nu_a(CH_2)$ = 2917 cm^{-1}. Frequencies related to asymmetric CH vibrations of the methyl terminal headgroup were assigned values of $\nu_a(CH_3,ip)$ = 2963 cm^{-1} and $\nu_a(CH_3,op)$ = 2955 cm^{-1}, where ip and op denote in-plane and out-of-plane stretching vibrations.[38] The band related the symmetric CH stretching mode in the methyl group is actually split into two modes resulting from Fermi resonance interactions, commonly denoted as $\nu_s(CH_3,FR)$, and have previously are observed at 2938 cm^{-1} and 2879 cm^{-1} in alkanethiol monolayers.[37,38]

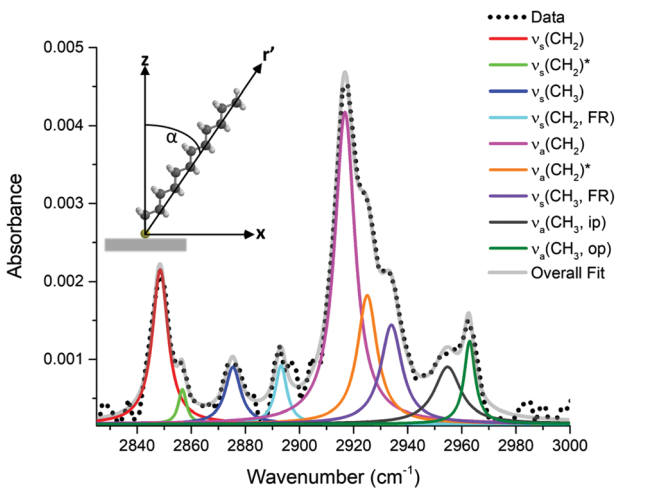

Fig. 2 Grazing angle IR absorbance spectrum of dodecanethiol, $CH_2(CH)_{11}S$/Ag (black dots), and a corresponding spectral deconvolution into various vibrational modes as shown in the legend and discussed in the text.

It is generally accepted that a well-defined SAM of *n*-alkanethiol chains on a flat surface will form a closely packed structure in the all-*trans* conformation with all of their alkyl chains forming a well-defined tilt angle, α, away from the surface normal as shown in inset of Fig. 2. The molecule can also be twisted along its molecular axis r' defined by the angle β. Previous works have shown that RAIRS can be used to estimate α on flat surfaces.[40] In RAIRS, a grazing angle of incidence is used, so the generated electric field is mostly perpendicular to the surface, and vibrational modes that have transition dipole moments parallel to the electric field are observed in IR spectra.[40] This forms a set of selection rules for molecules which have a preferential orientation. For the case of the *n*-alkyl thiols in the all-*trans* conformation, the transition dipole moment of the $\nu_s(CH_2)$ mode lies in the molecular plane, and is orthogonal to the molecular plane for an asymmetric stretch. The transition dipole moment for symmetric stretch in the methyl group, $\nu_s(CH_3)$, also lies in the molecular plane, oriented along the long axis of the molecule. Correspondingly, for α, $\beta = 0^\circ$, only the symmetric CH vibrations in the methyl group would be seen, whereas for $\alpha = 90^\circ$ and $\beta = 0^\circ$, only the symmetric CH vibrations in the methylene groups would be observed. In general, the chain tilt and twist angles are determined by fitting experimental results to a model capable of simulating experimental spectra for various values of α and β. However, on nano-textured metal surfaces that enable resonant coupling into plasmonic modes, the electric field may be oriented along several directions depending on the local nanostructure. The high topography of the surface will also influence the local orientation of the molecule. In this connection, there is a breakdown of the selection rules described above and the spectrum plotted in Fig. 2 can be deconvolved into all possible observable modes. The excellent agreement between the measured IR absorbance frequencies and the frequencies reported in the literature for closely packed *n*-alkyl thiols not only confirms that dodecanethiol is present on the Ag surfaces, but also suggests that the alkyl chains favour a *trans* conformation.[37]

Photooxidation of the dodecanethiol layer was initiated using an irradiance of 15 kW cm^{-2} (0.5 mW power) in a beam focussed through a 20×, 0.4 N.A. objective at a wavelength of 532 nm. The products of the reaction were monitored using Raman spectroscopy using the same laser. In contrast to previous works,[23,41,42] Raman scattering signals from C–C stretching modes in the thiol layer were not resolvable. A coloured silver sample that did not undergo the thiolation procedure, was also measured for comparison. Unlike the coloured silver surfaces, smooth bulk silver does not support surface plasmonic resonances, and therefore surface enhanced Raman scattering (SERS) effects cannot be observed, making it very difficult to obtain a measurable signal from any type of species which may be on

such a surface. In contrast, the plasmonic nature of the silver surface used in this study generates enhanced local electric fields[22,36] which amplify Raman scattering intensities. In keeping with this, previous studies in which Raman spectroscopy was used to study UV induced photooxidation of alkanethiol monolayers required the use of roughened silver substrates.[23] It is also instructive to note that quantitative analysis of any products or reactants can be very difficult to achieve due to highly localized and variable field intensities, commonly referred to as hotspots throughout the literature. From a qualitative perspective, Raman scattering signals provide strong evidence for the presence for molecular species of interest.

Raman spectra from the two samples (with and without the thiol layer), after 3 s and 1 h of exposure to the 532 nm laser are plotted in Fig. 3(a) and (b), respectively. During the first acquisition, neither sample generated any detectable Raman scattering signal. However, after 1 hour, clear spectral differences are seen between the samples. On surfaces where no dodecanethiol was present, a Raman spectrum that is relatively featureless is observed, whereas the irradiation of dodecanethiol on the coloured silver surface generates a spectrum containing high intensity narrowband lineshapes, and confirms that spectral differences result from the presence of the alkanethiol layer. Specifically, five new peaks centred at 470, 635, 711, 973, and 1190 cm^{-1} appear and are easily resolved in the spectrum, and represent the products of alkanethiol photooxidation that has taken place on the surface.[23–28] Time evolution Raman spectra over the course of one hour were recorded every minute and are plotted in Fig. 3(c). For the purpose of clarity, twelve spectra are plotted over five-minute intervals. One can see that the photooxidation process begins within the first five minutes of exposure. The most intense feature appearing in the 975 cm^{-1} region is assigned to the symmetric stretch of a sulfate (SO_4^{2-}) ion.[23,42] The peaks at 470, 635 and 1190 cm^{-1} are also assigned to Raman scattering from SO_4^{2-}, and follow the previous assignments in the literature.[23]

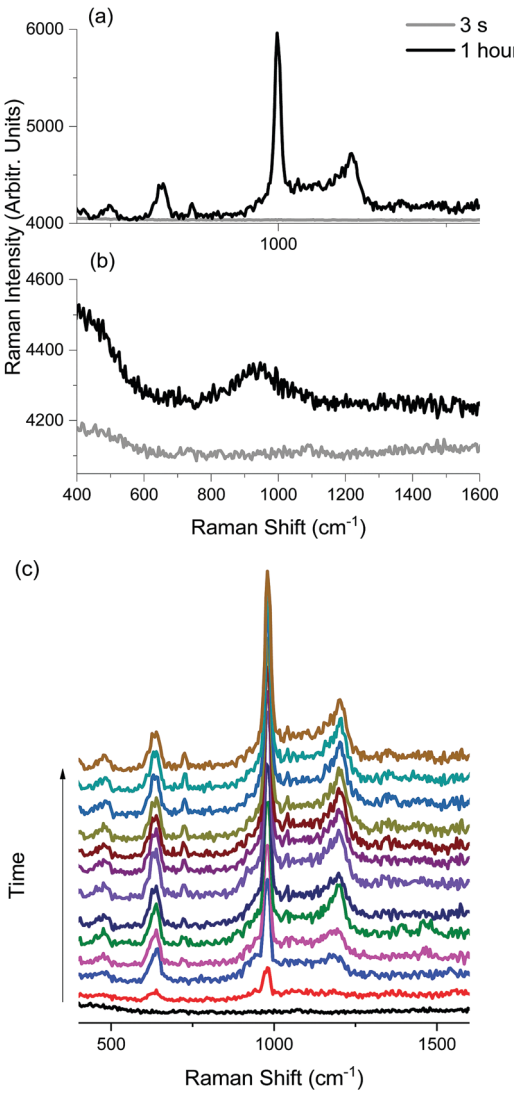

Fig. 3 Raman spectra after three seconds (grey traces) and 1 hour (black traces) of laser exposure from a silver surface with dodecanethiol (a) and without (b). Time evolution of the photooxidation process over the course of an hour (c).

Locally normalized Raman intensities as a function of time for the five peaks associated with scattering from sulphate species is shown in Fig. 4(a) for an incident power of 0.5 mW. All of the peaks essentially grow at the same rate, consistent with the assignment that they are all from the same surface species. The data were then fit to a single exponential, from which the rate was determined for each of the five peaks. The rates were then averaged to calculate a rate for a given incident power. This calculation was repeated for incident laser powers of 0.75, 1, 1.5, 2 and 2.5 mW and is plotted on a logarithmic scale in Fig. 4(b). The slope of this plots is $\sim$1.5 and suggests a strong non-linear dependence on light intensity. Generally, for a chemical reaction whose rate depends on temperature, a strong non-linear dependence of this type is expected.[43] Both thermal and hot carrier induced processes can generate various power laws.

Discussion

The observation of Raman scattering from sulfate species provides clear evidence that a chemical reaction takes places in areas which experienced laser irradiation, and suggests that the sulfur atom from the dodecanethiol layer remains bonded to the silver surface during the chemical transformation. This idea is supported by the fact that no evidence of any silver sulfate (Ag_2SO_4), silver sulfite (Ag_2SO_3) or silver sulfide (Ag_2S) was observed from surfaces which were not treated with dodecanethiol, and therefore the origin of sulfur was not from the surrounding environment. The lack of any signal from hydrocarbon units forming the tail end of the dodecanethiol molecule suggests that the molecule has been cleaved at the S–C bond. Cleaving of this bond has been previously reported in the literature[23,41] for SAMs of alkanethiols illuminated using UV light (photon energies $>$4.7 eV). It was proposed that photooxidation of alkanethiol species on silver under UV irradiation occurs *via* a two-step process.[23] First, C–S bond scission occurs

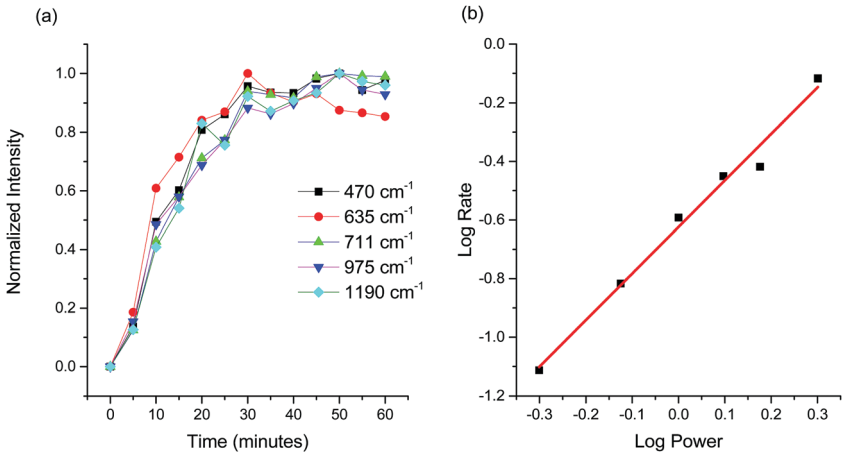

Fig. 4 (a) Locally normalized Raman scattering intensity as a function of time for each of the five peaks associated with Raman scattering from $SO4^{2-}$ units. (b) Average rate of reaction *versus* laser power on a logarithmic scale.

resulting in removal of the alkyl chain, after which oxidation of the exposed sulfur atoms proceeds. Expanding on this, another study has suggested that in addition to bond cleaving, a significant amount of alkylsulfonates were formed under UV excitation.[24] We did observe a contribution at 711 cm^{-1} from sulfite species, however since no scattering from units formatting the hydrocarbon were observed, this peak is tentatively assigned to Ag_2SO_3. Correspondingly, we assign the rest of the spectrum to Raman scattering from Ag_2SO_4.

Previous studies have attributed photooxidation of the S–C bond in alkanethiols on Ag to hot electron excitation.[23] In our study, the same chemical transformation is observed, but using a photon energy of only 2.33 eV. However, in contrast to previous literature on the subject, our surfaces consist of nano-textured silver supporting strongly localized plasmons in the visible, so care must be taken to understand their role in a photochemical reaction. Plasmonic excitations can decay non-radiatively by giving up their energy to carriers in the metal. These carriers can then be emitted into an adsorbate, thereby inducing a chemical reaction, or they can thermalize (heating of the lattice) with the resulting heat inducing a chemical reaction.

The silver surface used in this work exhibits a very strong optical absorptance in the visible which may lead to significant local heating of the sample surface. If indeed the observed chemical changes are driven by thermal effects, then identical chemical transformations should be observed when thermal energy only is supplied to the sample *via* resistive heating.[6] The results of such an experiment indicate that this is not the case. A sample was placed on a heating stage and raised to various temperatures ranging from 40 to 160 °C in 30 °C increments. Raman spectra were acquired at each temperature after 40 minutes of heating. Up to temperatures of 130 °C, all recorded Raman spectra were featureless, showing no evidence of sulfur compounds. Subjecting the sample to elevated temperatures did however significantly alter its colour. No colour changes were observed when samples were irradiated with the laser. It is instructive to note however, that the onset of thermal damage was found to occur when the irradiance was increased to 45–60 kW cm^{-2}. Based on these observations, the energy supplied for the observed S–C bond cleavage and subsequent photooxidation of the exposed sulfur atom is not thermal. This is somewhat expected since the nano-textured Ag surface is effectively in direct contact with a relatively large high purity (99.99%) Ag substrate which has a very high thermal conductivity of 429 W m^{-1} K^{-1}.[44]

Ruling out thermally-driven reactions, we now consider photochemistry involving charge carriers, specifically, what their role might be in cleaving the S–C bond in adsorbed dodecanethiol molecules. In understanding photochemistry on metal surfaces, the energies of the highest occupied molecular orbital (HOMO) and lowest unoccupied molecular orbital (LUMO) of the adsorbate molecule relative to the Fermi level of metallic surface is of central importance. In addition, if the metallic surface is nano-textured or consists of nanoparticles, then knowledge of LSPR frequencies and the corresponding enhancements in local electric field intensities are also required. Generally, when molecules adsorb onto metal surfaces, transition energies between the HUMO and LUMO level in the adsorbed molecule can be either blue- or red-shifted from their gas phase energies by as much as 1 eV. Lastly, these orbitals experience broadening when the metal–adsorbate complex forms and no longer consist of discrete energies. The HOMO–LUMO gap for adsorbed molecules on metal surfaces can be determined using scanning tunnelling microscopy (STM). In particular, the HOMO–LUMO gap for dodecanethiol has been reported to lie between ~7 to 8 eV.[21] The Fermi level of Ag is 4.3 eV and lies between the HOMO and LUMO levels of the adsorbed molecule.

Although the experimentally-measured HOMO–LUMO gap energies appearing in the literature for alkanethiol monolayers on gold and silver are consistent, the position of the Fermi energy with respect to these orbitals remains an open question. For example, conducting-probe atomic force microscopy (CP-AFM) measurements have shown that higher work function metals, such as Pt, decrease the contact resistance, and therefore barrier heights to tunnelling, compared to Au and Ag. It was

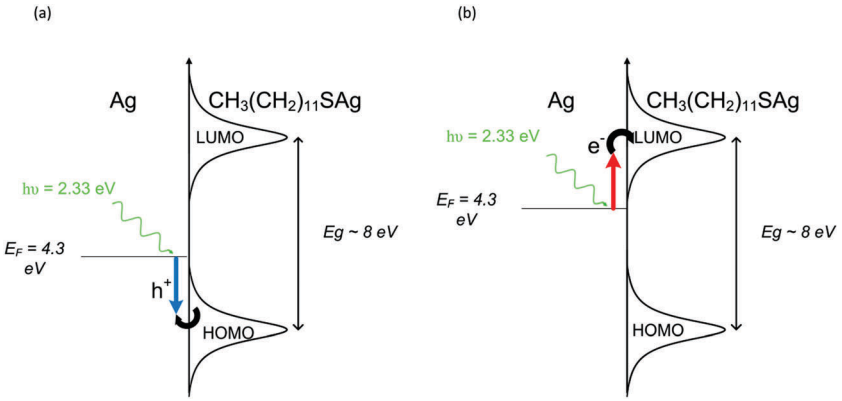

Fig. 5 Schematic of plasmon mediated charge transfer. Plasmons and photons with an energy of 2.33 eV generate hot holes (a) and hot electrons (b) over a range of energies. (a) Hot holes can capture electrons from occupied states (HOMO) in the molecule. (b) Excited electrons can tunnel into unoccupied electronic states in the molecule (LUMO). The direction of charge transfer in adsorbed dodecanethiol is unknown.

suggested that such trends are indicative that the Fermi level lies closer to the HOMO, and that charge transport is dominated by hole tunnelling.[45] On the other hand, the results of ultraviolet photoelectron spectroscopy (UPS) and inverse photoemission spectroscopy (IPES) experiments suggest that the main mechanism is electron tunneling and therefore the Fermi level is positioned closer to the LUMO.

When plasmons are excited on the surface of a metal, hot electrons and hot holes are created and become available to drive chemical reactions within the adsorbate. As shown in Fig. 5, excited carriers will be excited to a maximum energy of $h\nu$ above the Fermi level. Three mechanisms that lead to chemical transformations in adsorbed molecules are then possible: (i) a hot electron (Fig. 5a) can be excited from the Fermi level to the LUMO of the molecule. (ii) A hot hole (Fig. 5b) enables electron transfer to the metal from the HOMO of the adsorbate. These two scenarios are referred to as indirect adsorbate excitation, and generally require the corresponding frontier orbitals to lie near the Fermi level.[6] (iii) The coupling of surface plasmon energy into electronic states in the molecule enabling direct transitions is also possible.[7,8,43] In addition to this, an increasing number of reports are appearing in the literature discussing the effect of high intensity electric fields and increased charge-carrier yields.[12] Spaces between plasmonic nanostructures can generate higher intensity fields than on isolated nanoparticles and are thought to be areas of increased photochemical activity.

In our study, there are two reactions of interest. First, the cleaving of the S–C bond leading to the formation of silver sulfide, Ag_2S, followed by an oxidation reaction producing Ag_2SO_4. Quantum chemical calculations using time domain density functional theory (TDDFT) provide values for allowed UV/Vis transitions of molecules adsorbed on Ag clusters,[46] allowing to determine if charge transfer is from the metal to the molecule or *vice versa* for a given reaction. For example, theoretical calculations have shown that visible light driven reactions involving $ArNO_2$ on Ag clusters are due to electron transfer from silver to the LUMO of $ArNO_2$. On the other hand, it was also shown that electrons are transferred from the HOMO levels in adsorbed $ArNH_2$ molecules to unoccupied levels in silver.[47] Unfortunately, a detailed TDDFT calculation to confirm the direction of charge transfer for each reaction step is beyond the scope of this work. The experimental results demonstrate that the entire reaction can be driven with photon energies of 2.33 eV, and therefore the energy separation between the Fermi energy and either the HOMO or LUMO must lie within this energy range for bond cleaving to proceed, as sketched in Fig. 5. It is unlikely that the HOMO–LUMO energy gap for dodecanethiol would be reduced by $\sim$5 eV after adsorption, therefore direct excitation is ruled out. To our knowledge, this is the first demonstration of S–C bond scission in thiol molecules by visible light (532 nm radiation). The key to this reaction is a nano-textured Ag surface capable of strong absorption through SPR at visible wavelengths.

In addition to hot carriers, the reaction involving the oxidation of Ag_2S to Ag_2SO_4 requires the presence of oxygen species. From Fig. 4a, the Raman scattering intensity from sulfate species reaches a maximum after 20 minutes. Since an increase in reaction rate is observed as irradiance is increased, the limiting factor must be the concentration of hot carriers to drive the reaction forward and not molecular species in the surrounding environment. In previous works, alkanethiol oxidation on gold and silver surfaces in air, under UV excitation, required the presence of ozone (O_3).[48,49] It has been suggested that UV excitation leads to decomposition of O_3 into O_2 molecules in the singlet state. Oxygen molecules in the singlet state are known to be highly reactive. Plasmonic decomposition of O_3 has not been reported previously, and to assign the observed plasmonic photooxidation to ozone decomposition is premature; carefully designed experiments where the environment is controlled are required. Furthermore, metal sulfide oxidation will readily proceed in aqueous conditions, and therefore water molecules in the surrounding environment, or hydrogen bonded to the surface may play a role.

From a fabrication standpoint, laser machining represents a high throughput process capable of patterning large areas and requires minimal fabrication steps. When considering industrial scale operations, these attributes are essential if

the technology is eventually going to scale-up. On the other hand, nanofabrication tools like electron beam lithography and focused ion beam milling can produce extremely well-defined structures at the nanoscale to support strong optical resonances in the visible range. This in turn would lower the power input requirement to initiate photooxidation. Self-assembled plasmonic silver structures with tunable resonances have also been realized,[50] and can be fabricated over large areas as well. Along these lines, the best fabrication tool for photochemical applications involving silver remains an open question and requires further investigation.

Conclusions

We demonstrated that plasmonic resonances in the visible can be used to drive photochemical reactions on nano-textured silver. Specifically, it was found that hot carriers in silver, of maximum excess energy of 2.33 eV (corresponding to irradiation with 532 nm light), are responsible for cleaving the S–C bond, and the subsequent desorption of alkyl chains, in adsorbed dodecanethiol. It is also proposed that hot carriers are responsible for the rapid oxidation of the exposed sulfur atom, however it is unclear if ozone decomposition plays a role. Photochemical transformations on plasmonic metal surfaces is a relatively new field. The large-area, easy to fabricate, nano-textured silver substrates capable of photochemical activity will enable researchers in many different fields to examine plasmon-assisted chemical processes in greater detail. In general, the ability to drive reactions with visible light instead of UV light (as used in past work, *e.g.*, on dodecanethiol) is significant, as visible light is safer due to the lower photon energy involved, and inexpensively generated, detected and managed.

Conflicts of interest

There are no conflicts to declare.

Acknowledgements

We would like to thank the Royal Canadian Mint for providing high purity silver samples, access to laser micro-machining facilities, and for their gracious financial support. We also thank Daniel Poitras from the National Research Council of Canada for acquiring the reflectance spectrum. We acknowledge the Natural Sciences and Engineering Research Council of Canada, the Canada Research Chairs program, and the Ontario Ministry of Research and Innovation (MRI) through the Leaders of Opportunity (LOF) fund.

References

1 A. J. Haes and R. P. Van Duyne, A nanoscale optical biosensor: sensitivity and selectivity of an approach based on the localized surface plasmon resonance spectroscopy of triangular silver nanoparticles, *J. Am. Chem. Soc.*, 2002, **124**(35), 10596–10604.
2 E. Hutter and J. H. Fendler, Exploitation of localized surface plasmon resonance, *Adv. Mater.*, 2004, **16**(19), 1685–1706.
3 K. A. Willets and R. P. Van Duyne, Localized surface plasmon resonance spectroscopy and sensing, *Annu. Rev. Phys. Chem.*, 2007, **58**, 267–297.
4 J. N. Anker, W. P. Hall, O. Lyandres, N. C. Shah, J. Zhao and R. P. Van Duyne, Biosensing with plasmonic nanosensors, *Nat. Mater.*, 2008, **7**(6), 442–453.
5 Y. Liu, Q. Liu, S. Chen, F. Cheng, H. Wang and W. Peng, Surface plasmon resonance biosensor based on smart phone platforms, *Sci. Rep.*, 2015, **5**, 12864.
6 S. Linic, U. Aslam, C. Boerigter and M. Morabito, Photochemical transformations on plasmonic metal nanoparticles, *Nat. Mater.*, 2015, **14**(6), 567.
7 C. Boerigter, R. Campana, M. Morabito and S. Linic, Evidence and implications of direct charge excitation as the dominant mechanism in plasmon-mediated photocatalysis, *Nat. Commun.*, 2016, **7**, 10545.
8 C. Boerigter, U. Aslam and S. Linic, Mechanism of charge transfer from plasmonic nanostructures to chemically attached materials, *ACS Nano*, 2016, **10**(6), 6108–6115.
9 S. Aslam Mukherjee, F. Libisch, N. Large, O. Neumann, L. V. Brown, J. Cheng, J. B. Lassiter, E. A. Carter, P. Nordlander and N. J. Halas, Hot electrons do the impossible: plasmon-induced dissociation of H2 on Au, *Nano Lett.*, 2013, **13**(1), 240–247.
10 Y. Kim, D. Dumett Torres and P. K. Jain, Activation Energies of Plasmonic Catalysts, *Nano Lett.*, 2016, **16**(5), 3399–3407.
11 L. Vazquez Besteiro, X. T. Kong, Z. Wang, G. V. Hartland and A. O. Govorov, Understanding Hot-Electron Generation and Plasmon Relaxation in Metal Nanocrystals: Quantum and Classical Mechanisms, *ACS Photonics*, 2017, **4**(11), 2759–2781.
12 M. L. Brongersma, N. J. Halas and P. Nordlander, Plasmon-induced hot carrier science and technology, *Nat. Nanotechnol.*, 2015, **10**(1), 25–34.
13 S. S. Acimovic, M. P. Kreuzer, M. U. González and R. Quidant, Plasmon near-field coupling in metal dimers as a step toward single-molecule sensing, *ACS Nano*, 2009, **3**(5), 1231–1237.
14 P. J. Schuck, D. P. Fromm, A. Sundaramurthy, G. S. Kino and W. E. Moerner, Improving the mismatch between light and nanoscale objects with gold bowtie nanoantennas, *Phys. Rev. Lett.*, 2005, **94**(1), 017402.
15 D. K. Lim, K. S. Jeon, H. M. Kim, J. M. Nam and Y. D. Suh, Nanogap-engineerable Raman-active nanodumbbells for single-molecule detection, *Nat. Mater.*, 2010, **9**(1), 60.
16 D. K. Lim, K. S. Jeon, J. H. Hwang, H. Kim, S. Kwon, Y. D. Suh and J. M. Nam, Highly uniform and reproducible surface-enhanced Raman scattering from DNA-tailorable nanoparticles with 1 nm interior gap, *Nat. Nanotechnol.*, 2011, **6**(7), 452–460.
17 S. Datta, W. Tian, S. Hong, R. Reifenberger, J. I. Henderson and C. P. Kubiak, Current-voltage characteristics of self-assembled monolayers by scanning tunneling microscopy, *Phys. Rev. Lett.*, 1997, **79**(13), 2530.

18 G. E. Poirier, Characterization of organosulfur molecular monolayers on Au (111) using scanning tunneling microscopy, *Chem. Rev.*, 1997, **97**(4), 1117–1128.
19 N. Okabayashi, Y. Konda and T. Komeda, Inelastic electron tunneling spectroscopy of an alkanethiol self-assembled monolayer using scanning tunneling microscopy, *Phys. Rev. Lett.*, 2008, **100**(21), 217801.
20 D. J. Wold and C. D. Frisbie, Formation of metal–molecule–metal tunnel junctions: microcontacts to alkanethiol monolayers with a conducting AFM tip, *J. Am. Chem. Soc.*, 2000, **122**(12), 2970–2971.
21 A. Salomon, D. Cahen, S. Lindsay, J. Tomfohr, V. B. Engelkes and C. D. Frisbie, Comparison of electronic transport measurements on organic molecules, *Adv. Mater.*, 2003, **15**(22), 1881–1890.
22 J. M. Guay, A. C. Lesina, G. Côté, M. Charron, D. Poitras, L. Ramunno, P. Berini and A. Weck, Laser-induced plasmonic colours on metals, *Nat. Commun.*, 2017, **8**, 16095.
23 M. Lewis, M. Tarlov and K. Carron, Study of the photooxidation process of self-assembled alkanethiol monolayers, *J. Am. Chem. Soc.*, 1995, **117**(37), 9574–9575.
24 D. A. Hutt and G. J. Leggett, Influence of adsorbate ordering on rates of UV photooxidation of self-assembled monolayers, *J. Phys. Chem.*, 1996, **100**(16), 6657–6662.
25 E. Cooper and G. J. Leggett, Static secondary ion mass spectrometry studies of self-assembled monolayers: influence of adsorbate chain length and terminal functional group on rates of photooxidation of alkanethiols on gold, *Langmuir*, 1998, **14**(17), 4795–4801.
26 N. J. Brewer, S. Janusz, K. Critchley, S. D. Evans and G. J. Leggett, Photooxidation of self-assembled monolayers by exposure to light of wavelength 254 nm: a static SIMS study, *J. Phys. Chem. B*, 2005, **109**(22), 11247–11256.
27 C. Zhou and A. V. Walker, UV photooxidation and photopatterning of alkanethiolate self-assembled monolayers (SAMs) on GaAs (001), *Langmuir*, 2007, **23**(17), 8876–8881.
28 H. Rieley, N. J. Price, T. L. Smith and S. Yang, Photooxidation and photo-reduction in alkylthiol monolayers self-assembled on gold, *J. Chem. Soc., Faraday Trans.*, 1996, **92**(19), 3629–3634.
29 S. Sun, K. S. Chong and G. J. Leggett, Nanoscale molecular patterns fabricated by using scanning near-field optical lithography, *J. Am. Chem. Soc.*, 2002, **124**(11), 2414–2415.
30 A. Kumar, N. L. Abbott, H. A. Biebuyck, E. Kim and G. M. Whitesides, Patterned self-assembled monolayers and meso-scale phenomena, *Acc. Chem. Res.*, 1995, **28**(5), 219–226.
31 Y. Xia, X. M. Zhao and G. M. Whitesides, Pattern transfer: Self-assembled monolayers as ultrathin resists, *Microelectron. Eng.*, 1996, **32**(1–4), 255–268.
32 M. J. Tarlov, D. R. Burgess Jr and G. Gillen, UV photopatterning of alkanethiolate monolayers self-assembled on gold and silver, *J. Am. Chem. Soc.*, 1993, **115**(12), 5305–5306.
33 J. C. Valmalette, Z. Tan, H. Abe and S. Ohara, Raman scattering of linear chains of strongly coupled Ag nanoparticles on SWCNTs, *Sci. Rep.*, 2014, **4**, 5238.
34 I. Martina, R. Wiesinger and M. Schreiner, Micro-Raman investigations of early stage silver corrosion products occurring in sulfur containing atmospheres, *J. Raman Spectrosc.*, 2013, **44**(5), 770–775.
35 J. M. Guay, A. C. Lesina, J. Baxter, M. Charron, G. Côté, L. Ramunno, P. Berini and A. Weck, Enhanced plasmonic coloring of silver and formation of large laser-induced periodic surface structures using multi-burst picosecond pulses, 2016, arXiv:1609.04847 arXiv preprint.
36 J. Jandeleit, G. Urbasch, H. D. Hoffmann, H. G. Treusch and E. W. Kreutz, Picosecond laser ablation of thin copper films, *Appl. Phys. A: Mater. Sci. Process.*, 1996, **63**(2), 117–121.
37 P. E. Laibinis, G. M. Whitesides, D. L. Allara, Y. T. Tao, A. N. Parikh and R. G. Nuzzo, Comparison of the structures and wetting properties of self-assembled monolayers of n-alkanethiols on the coinage metal surfaces, copper, silver, and gold, *J. Am. Chem. Soc.*, 1991, **113**(19), 7152–7167.
38 M. D. Porter, T. B. Bright, D. L. Allara and C. E. Chidsey, Spontaneously organized molecular assemblies. 4. Structural characterization of *n*-alkyl thiol monolayers on gold by optical ellipsometry, infrared spectroscopy, and electrochemistry, *J. Am. Chem. Soc.*, 1987, **109**(12), 3559–3568.
39 M. J. Hostetler, J. J. Stokes and R. W. Murray, Infrared spectroscopy of three-dimensional self-assembled monolayers: N-alkanethiolate monolayers on gold cluster compounds, *Langmuir*, 1996, **12**(15), 3604–3612.
40 R. E. Tim, Ageing of alkanethiol self-assembled monolayers, *J. Chem. Soc., Faraday Trans.*, 1996, **92**(23), 4759–4762.
41 C. J. Sandroff and D. R. Herschbach, Surface-enhanced Raman study of organic sulfides adsorbed on silver: facile cleavage of sulfur-sulfur and carbon-sulfur bonds, *J. Phys. Chem.*, 1982, **86**(17), 3277–3279.
42 K. L. Kim, S. J. Lee and K. Kim, Surface-enhanced Raman scattering of benzyl phenyl sulfide in silver sol: excitation-wavelength-dependent surface-induced photoreaction, *J. Phys. Chem. B*, 2004, **108**(26), 9216–9220.
43 X. L. Zhou, X. Y. Zhu and J. M. White, Photochemistry at adsorbate/metal interfaces, *Surf. Sci. Rep.*, 1991, **13**(3-6), 73–220.
44 W. J. Parker, R. J. Jenkins, C. P. Butler and G. L. Abbott, Flash method of determining thermal diffusivity, heat capacity, and thermal conductivity, *J. Appl. Phys.*, 1961, **32**(9), 1679–1684.
45 J. M. Beebe, V. B. Engelkes, L. L. Miller and C. D. Frisbie, Contact resistance in metal−molecule−metal junctions based on aliphatic SAMs: effects of surface linker and metal work function, *J. Am. Chem. Soc.*, 2002, **124**(38), 11268–11269.
46 C. Jamorski Jödicke and H. P. Lüthi, Time-Dependent Density Functional Theory (TDDFT) Study of the Excited Charge-Transfer State Formation of a Series of Aromatic Donor−Acceptor Systems, *J. Am. Chem. Soc.*, 2003, **125**(1), 252–264.
47 L. B. Zhao, Y. F. Huang, X. M. Liu, J. R. Anema, D. Y. Wu, B. Ren and Z. Q. Tian, A DFT study on photoinduced surface catalytic coupling reactions on nano-textured silver:

selective formation of azobenzene derivatives from para-substituted nitrobenzene and aniline, *Phys. Chem. Chem. Phys.*, 2012, **14**(37), 12919–12929.

48 Y. Zhang, R. H. Terrill, T. A. Tanzer and P. W. Bohn, Ozonolysis is the primary cause of UV photooxidation of alkanethiolate monolayers at low irradiance, *J. Am. Chem. Soc.*, 1998, **120**(11), 2654–2655.

49 M. H. Schoenfisch and J. E. Pemberton, Air stability of alkanethiol self-assembled monolayers on silver and gold surfaces, *J. Am. Chem. Soc.*, 1998, **120**(18), 4502–4513.

50 X. Y. Zhang, A. Hu, T. Zhang, W. Lei, X. J. Xue, Y. Zhou and W. W. Duley, Self-assembly of large-scale and ultrathin silver nanoplate films with tunable plasmon resonance properties, *ACS Nano*, 2011, **5**(11), 9082–9092.